Exploring diffusion in 4D near-the-Id symplectic maps

TraX 2022

Barcelona, 11-12/05/2022.

Arturo Vieiro [a]

vieiro@maia.ub.es

Universitat de Barcelona

Departament de Matemàtiques i Informàtica

[a]Joint work with V.Gelfreich (Univ. Warwick, UK).

4D near-the-identity maps

For concreteness [a] we consider a 4D near-the-identity symplectic maps that are obtained as a discretization of 2-dof Hamiltonian flows. That is:

Given $H : \mathbb{R}^2 \times \mathbb{T}^2 \simeq \mathbb{R}^2/\mathbb{T}^2 \to \mathbb{R}$ of the form $H(J,\psi) = T(J) + V(\psi)$,

$$T(J) = J_1^2/2 + a_2 J_1 J_2 + a_3 J_2^2/2, \qquad \text{with} \quad a_3 - a_2^2 > 0,$$

we associate to it the family of symplectic 4D maps F_δ given by

$$F_\delta(\psi, J) = (\bar{\psi}, \bar{J}) = \left(\psi + \delta\omega(\bar{J}), J - \delta g(\psi)\right),$$

where $\omega(J) = DT(\bar{J}),\ g(\psi) = DV(\psi)$.

By introducing $I = \delta J$ and $\epsilon = \delta^2$ we obtain

$F_\epsilon(\psi, I) = (\bar{\psi}, \bar{I}) = \left(\varphi + \omega(\bar{I}), I - \epsilon g(\psi)\right)$, hence F_0 is an integrable twist, and $\omega(I)$ the corresponding frequency vector.

Resonances: $\{k \in \mathbb{Z}^2 : k \cdot w(I) = 0\}$

[a] even though the theory can be adapted to a more general setting, our examples will be of this form

A concrete example

We consider near-the-Id 4D symplectic maps of the cylinder $M = \mathbb{T}^2 \times \mathbb{R}^2$.
As a concrete example, consider

$$T_\delta : \begin{pmatrix} \psi_1 \\ \psi_2 \\ J_1 \\ J_2 \end{pmatrix} \mapsto \begin{pmatrix} \bar{\psi}_1 \\ \bar{\psi}_2 \\ \bar{J}_1 \\ \bar{J}_2 \end{pmatrix} = \begin{pmatrix} \psi_1 + \delta(\bar{J}_1 + a_2 \bar{J}_2) \\ \psi_2 + \delta(a_2 \bar{J}_1 + a_3 \bar{J}_2) \\ J_1 - \delta \sin(\psi_1) \\ J_2 - \delta\epsilon \sin(\psi_2) \end{pmatrix}$$

where $a_2, a_3, \delta, \epsilon$ are real parameters ($a_2 = \epsilon = 0.5$ and $a_3 = 1.25$).

It was derived [a] as a **first order model for the dynamics at a double resonance** (crossing of two resonances of similar but different order) when unfolding the dynamics from a doubly resonant totally elliptic fixed point.

The symmetries of this map imply that not all the harmonics of the potential V appear in its Fourier expansion. More general maps will be considered later.

[a] V.Gelfreich, C.Simó and AV, *Dynamics of 4D symplectic maps near a double resonance*, Physica D 243, 2013.

Numerical evidence

Diffusion along phase space takes place basically along single resonances but multiple resonances play a key role in an explanation of the Arnold diffusion (e.g. Nekhoroshev theory – upper bounds on the rate of diffusion).

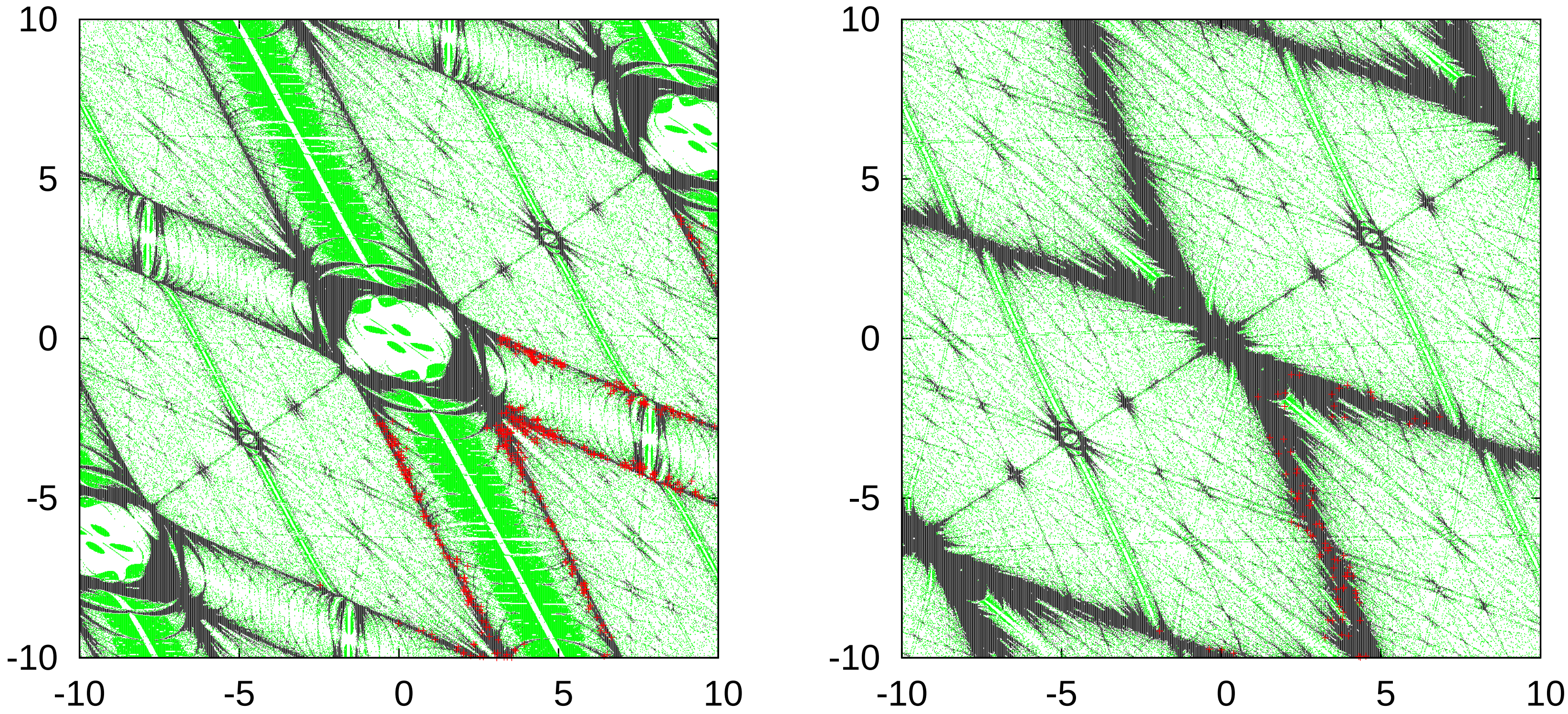

$\delta = \epsilon = a_2 = 0.5$, $a_3 = 1.25$. Lyap. exp. (megno): **black** $\rightarrow$ chaotic, green $\rightarrow$ weakly chaotic, white $\rightarrow$ regular. Red: Iterates of the point $(0, 0, 4.5, -5.25)$ in a slice of width 5×10^{-3} around $\psi_1 = \psi_2 = 0$ (left plot) and $\psi_1 = \psi_2 = \pi$ (right plot). Total number of iterates=10^{12}.

Relation with 3-dof Hamiltonian flows

The map F_ϵ is the isoenergetic Poincaré return map to $\Sigma_0 = \{\phi_3 = 0\} \cap \{H(I, I_3, \phi, \phi_3) = 0\}$ associated to the analytic 3-dof Hamiltonian flow that defines [a]

$$\hat{H}(\hat{I}, \hat{\psi}, \epsilon) = \hat{H}_0(\hat{I}) + \epsilon \hat{H}_1(I, \hat{\phi}, \epsilon), \text{ where}$$

$\hat{I} = (I, I_3)$, $\hat{\psi} = (\psi, \psi_3)$, $\hat{w}(\hat{I}) = (w(I), 1)$ and $H_0(\hat{I}) = \hat{\omega}(\hat{I}) \cdot \hat{I}$,

The Hamiltonian $\hat{H}$ is a quasi-integrable analytic Hamiltonian:

1. KAM theory provides 3D tori that do not divide the 5D energy level leading (generically) to instability for arbitrary small perturbations (Arnold diffusion).
2. Nekhoroshev theory provides stability for exponentially long times with respect to the inverse of the perturbation parameter ϵ (effective stability).

Goal: Investigate the Arnold diffusion process for the "equivalent" map F_δ and to study the role of double resonances in the (Arnold) diffusion.

[a] S.Kuksin and J.Pöschel, *On the inclusion of analytic symplectic maps in analytic Hamiltonian flows and its applications.* Seminar on Dynamical Systems 12:96–116, 1994

Geometric part of Nekhoroshev theorem

The role of double resonances is emphasized in the proof of Nekhoroshev theorem by Lochak-Neishtadt [a]. Note that $\hat{H}_0$ is quasiconvex (level surfaces are convex) since $a_3 - a_2^2 > 0$.

The mains steps of the proposed proof of Nekhoroshev estimates consist in

1. Construct a covering of the action space by open neighbourhoods of a finite number (depending on ϵ) of periodic orbits (maximum resonances) of $\hat{H}_0$.
2. Normalize the Hamiltonian around a periodic orbit: by successive changes of variables (averaging procedure) the non-resonant terms of $\hat{H}$ can be annihilated within an exponentially small error.
3. Use **convexity** to guarantee exponential stability in the neighbourhood.

[a] P.Lochak and A.I.Neishtadt, *Estimates of stability time for nearly integrable systems with a quasiconvex Hamiltonian*, Chaos 2, 1992.

Adapting the result for near-Id 4D maps

The first step of Lochak-Neishtadt result adapted to our “map setting” (i.e. one of the frequencies is fixed to 1) shows that one can cover the action space of F_δ by considering the N-periodic orbits up to period $N_{\max} \sim \epsilon^{-1/3}$ and consider a neighbourhood of radius $\sim \frac{1}{N}\epsilon^{1/6}$ around. $\leftarrow$ “influence radius”

Then, by normalizing the Hamiltonian in each neighbourhood one obtains:

$$\forall (I_0, \psi_0) \in \mathbb{T}^2 \times \mathbb{R}^2, |I(t) - I_0| < c\epsilon^{1/6} \text{ for } t \lesssim \exp(\tilde{c}\,\epsilon^{1/6}).$$

Remarks:

1. Arnold diffusion has to do with the propagation of the slowest variable of the system. By contrast, Nekhoroshev theorem deals with the effective stability of the former first integrals of F_0 (the two actions!).
2. If initial conditions are taken $\mathcal{O}(\sqrt{\epsilon})$-close to the double resonance the estimates can be improved: actions change by no more that $\mathcal{O}(\sqrt{\epsilon})$ over a time $T = \exp(c/\sqrt{\epsilon})$. $\leftarrow$ “core radius”, much longer time scale!!

Numerics - Some questions & difficulties

We want to investigate phase space of F_δ for a fixed small value of δ.
Explorations show that iterates of ICs travel along single resonances in phase space and visit neighbourhoods of different double resonances. Hence, to elucidate the diffusive process, we have to explore a large region of the phase space for many ICs.

- Can we determine the "optimal" covering of phase space?
- Can we evaluate the slowest variable at any point of the phase space? In particular, can we avoid the change of coordinates leading to a normalization of the Hamiltonian around each of the periodic orbits at the important double resonances?
- Can we investigate the neighbourhood of a double resonances? Determine different expected behaviours of iterates?

We believe that our numerical investigations, that extensively use the so-called interpolating vector fields (IVFs), provide some intuition on the previous items.

IVFs - a tool to study near-Id dynamics

Consider a smooth one-parameter near identity family of maps $F_\epsilon : D \to \mathbb{R}^m$ where $m \geq 1$, $D \subset \mathbb{R}^m$ is an open domain and $|\epsilon| < \epsilon_0$. It can be written as

$$F_\epsilon(x) = x + \epsilon\, G_\epsilon(x).$$

Fix $n \in \mathbb{N}$. Given $x \in D$, consider $x_k = F_\epsilon^k(x) \in D$ for $|k| \leq n$. Then, $\exists!$ polynomial $p_n \in \mathcal{P}_{2n}(t)$ s.t. $x_k = p_n(t_k; x_0, \epsilon)$, $\forall t_k = \epsilon k$, $|k| \leq n$.

Definition. The interpolating vector field (IVF) X_n at $x \in D$ is the velocity vector of the interpolating curve at $t = 0$, that is, $X_n(x, \epsilon) = \partial_t p_n(0, x, \epsilon)$.

1. X_n extends continuously to $\epsilon = 0$ and $X_n(x, 0) = G_0(x)$ the limit v.f.
2. The IVF X_n is a linear combination of the iterates of x:

$$X_n(x,\epsilon) = \epsilon^{-1} \sum_{k=-n}^{n} p_{nk} x_k = \epsilon^{-1} \sum_{k=1}^{n} p_{nk}(x_k - x_{-k}),$$

where

$$p_{nk} = \frac{(-1)^{k+1}(n!)^2}{k(n+k)!(n-k)!}, \quad 1 \leq |k| \leq n.$$

IVFs - Suspension + averaging

Rec. A suspension of F_ϵ is a time-periodic vector field Y such that $\Phi^1_\epsilon = F_\epsilon$ (interpolates).

By successive averaging steps one can get a suspension Y as close to an autonomous vector field as possible. For example, if Y analytic in a complex neighbourhood of D then after $n \sim |\epsilon|^{-1}$ steps one gets $Y(\tau, x, \epsilon) = A(x, \epsilon) + B(\tau, x, \epsilon)$, with $B = O(\exp(-c/|\epsilon|))$ for some $c > 0$.

Theorem (Gelfreich-V, 2018). [a] If a suspension of F_ϵ can be written as

$$Y(t, x, \epsilon) = A_n(x, \epsilon) + \epsilon^{2n} B_n(t, x, \epsilon)$$

where the $\mathcal{C}^{2n}$ norms of A_n and B_n are bounded uniformly with respect ϵ, then for every compact $D_0 \subset D$ there is a constant C_n such that

$$\sup_{x \in D} |A_n(x, \epsilon) - X_n(x, \epsilon)| \leq C_n \epsilon^{2n}$$

where X_n is the interpolating vector field for the map F_ϵ.

---

[a] V.Gelfreich and AV, *Interpolating vector fields for near identity maps and averaging*, Nonlinearity 31(9), 4263–4289, 2018

F_ϵ *is close to the time-*ϵ *flow of the IVF*

From the previous result it follows the following

Corollary. If $F_\epsilon \in \mathcal{C}^{2n+1}$ and $D_0 \subset D$ compact, then the IVF X_n is uniformly bounded in D_0 for $|\epsilon| < \epsilon_0$ and

$$F_\epsilon(x) = \Phi^\epsilon_{X_n}(x) + O(|\epsilon|^{2n+1}).$$

Corollary. If F_ϵ is analytic in a complex neighbourhood of D_0 then we can choose $n \sim |\epsilon|^{-1}$ in order to obtain a vector field which interpolates F_ϵ with an error exponentially small in ϵ,

$$F_\epsilon(x) = \Phi^\epsilon_{X_n}(x) + O(\exp(-c/|\epsilon|)),\ c > 0.$$

For example, for $n = 1$ the error is $\mathcal{O}(|\epsilon|^3)$, better than the limit flow G_0.

Example: Chirikov standard map on $\mathbb{S}^1 \times \mathbb{R}$

$$M_\epsilon : (x, y) \mapsto (\bar{x}, \bar{y}) = (x + \epsilon\bar{y}, y - \epsilon \sin(x)), \quad \epsilon \in \mathbb{R}.$$

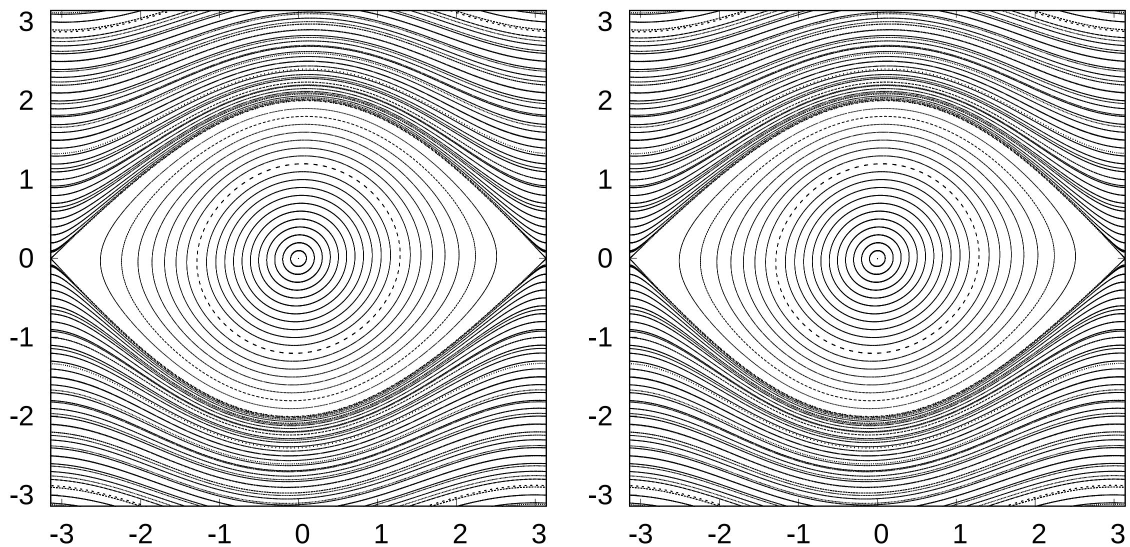

$\epsilon = 0.1$, same 200 i.c.

Left: 10^3 iterates of M_ϵ.

Right: RK78 integration of X_5 up to $t = 10^3$ plotting every $\Delta t = 0.1$.

No visual differences!

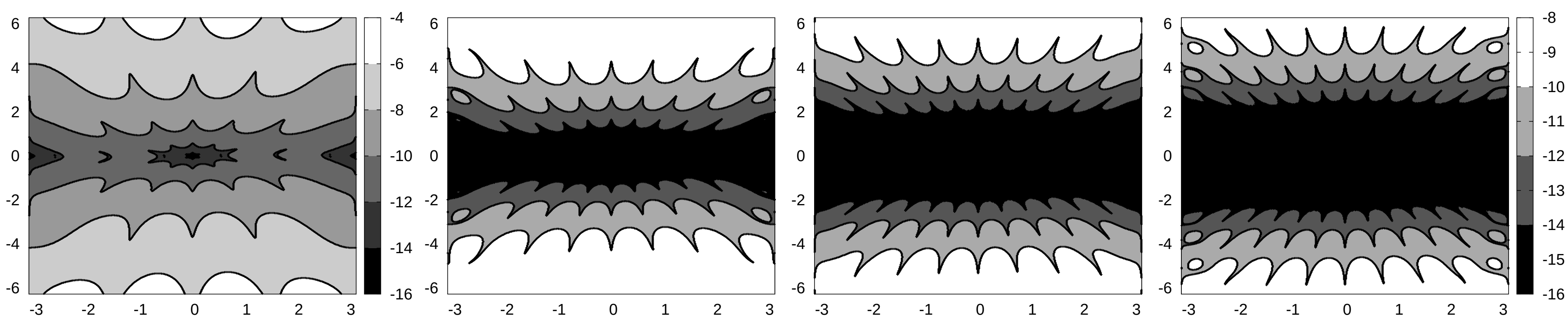

Level plots of $\log_{10} |\Phi^\epsilon_{X_n}(x) - M_\epsilon(x)|$ for $n = 5, 10, 15, 20.$

Example: M_ϵ vs. X_{10}, $\epsilon = 0.5$

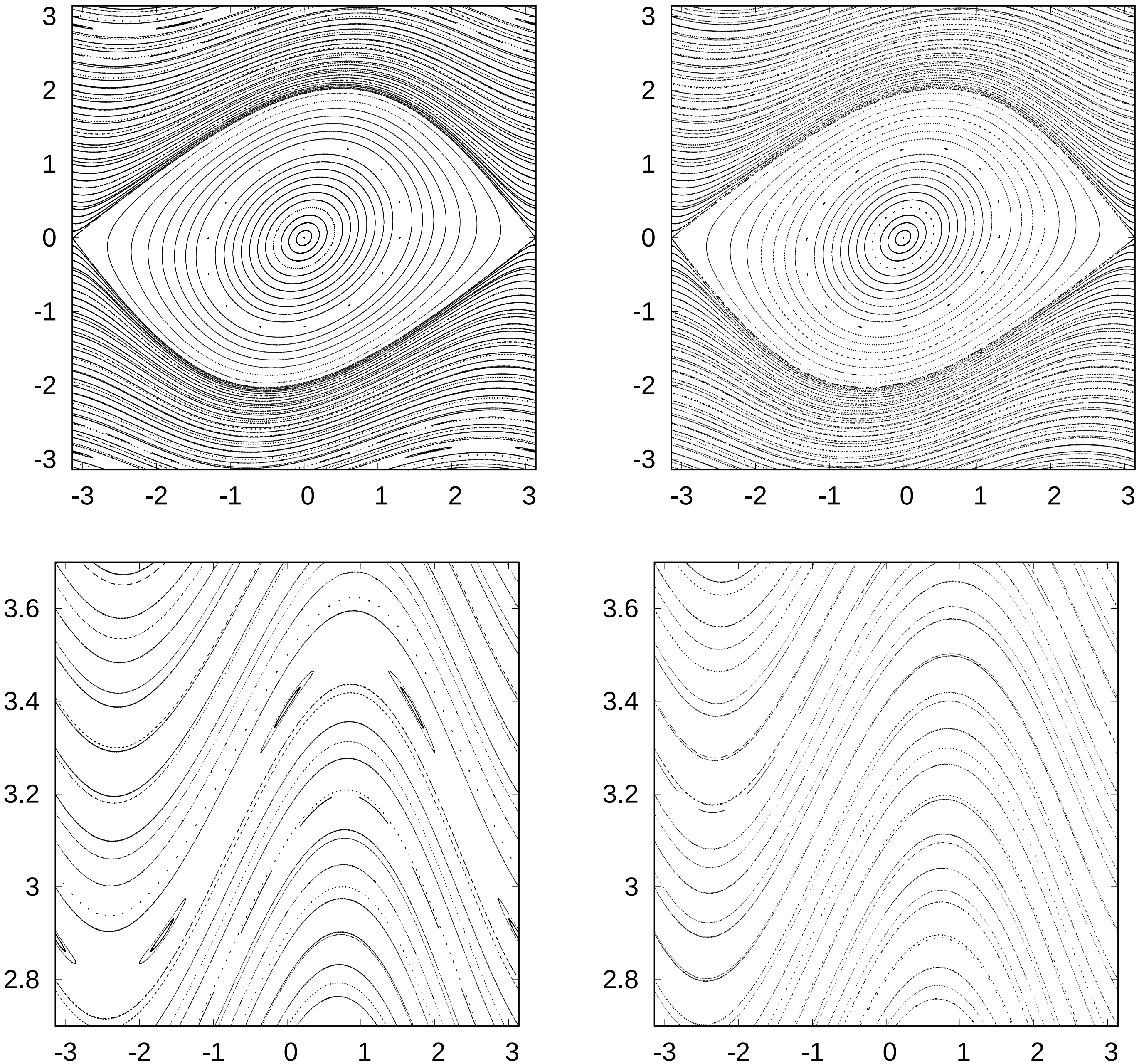

Remark:

F_ϵ reversible + 2D

$\Downarrow$

X_n reversible

$\Downarrow$

X_n foliated by p.o.

$\Downarrow$

X_n Hamiltonian

(non-standard

symplectic form)

Example: Dissipative standard map

$$M_{\epsilon,\delta} : (x, y) \mapsto (\bar{x}, \bar{y}) = (x + \delta \bar{y}, (1 - \epsilon)y - \delta \sin(2\pi x) + c), \quad \epsilon \in \mathbb{R}.$$

We consider $\delta \approx 3.57 \times 10^{-1}, \omega \approx 6.18 \times 10^{-1}$ and $\epsilon = 10^{-2}$ (left), $10^{-3} (center/right)$.

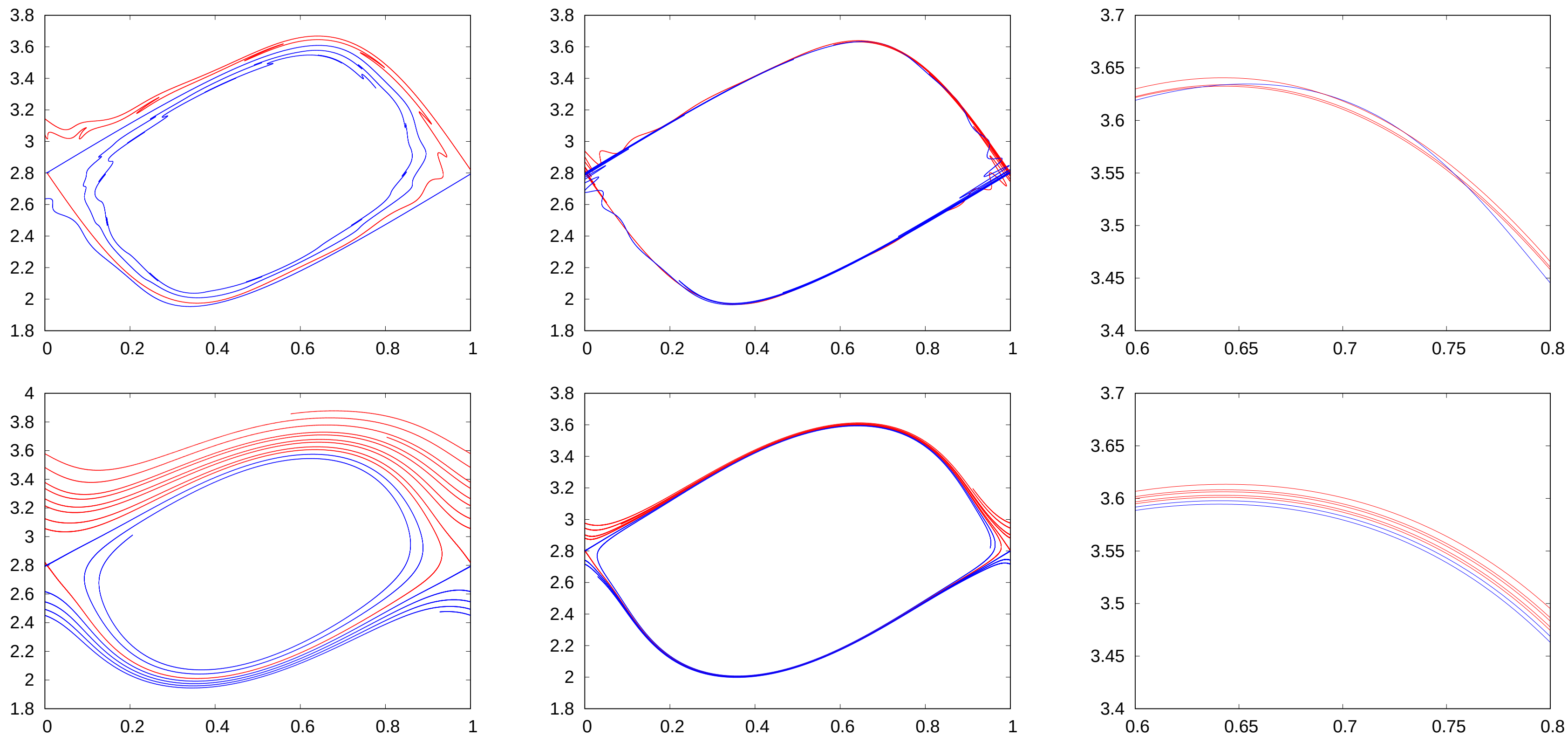

The origin is an attracting focus. Preliminary numerical exploration indicate that the probability of capture by the focus can be defined as the ratio between the entrance/exit strips (one can avoid homoclinics).

IVFs - near-Id symplectic maps

IVFs can be used to construct an adiabatic invariant of a symplectic near-Id map F_ϵ. Consider $m = 2d$, $\omega = \sum_{i=1}^{d} dx_i \wedge dx_{i+d}$ symplectic form, $F_\epsilon^*(\omega) = \omega$. Then the IVF X_n is close to a Hamiltonian flow.

Let $\nu_n = \omega(X_n, \cdot) = \sum_{1\le i\le d} \left(X_n^i dx_{i+d} - X_n^{i+d} dx_i\right)$, where $X_n = (X_n^i)_{i=1,\dots,m}$. Given $p_0 \in D$ define for every $x \in D$

$$h_n^\epsilon(x; p_0) = \int_{\gamma(p_0,x)} \nu_n \ , \qquad \text{along a path } \gamma(p_0, x) \text{ from } p_0 \text{ to } x.$$

Lemma (Gelfreich-V, 2022). Consider F_ϵ defined on $\mathbb{T}^2 \times \mathbb{R}^2$ and assume that h_n is computed along a piecewise path with straight segments parallel to the (ordered) axes. Then, there is a constant c_1 and a periodic function c_2 such that

$$\tilde{h}_n(x; p_0) = h_n(x; p_0) - c_1(x^0 - p_0^0) - c_2(x^0)(x_1 - p_0^1),$$

is globally well-defined on $\mathbb{T}^2 \times \mathbb{R}^2$.

Correction of h_n to be periodic

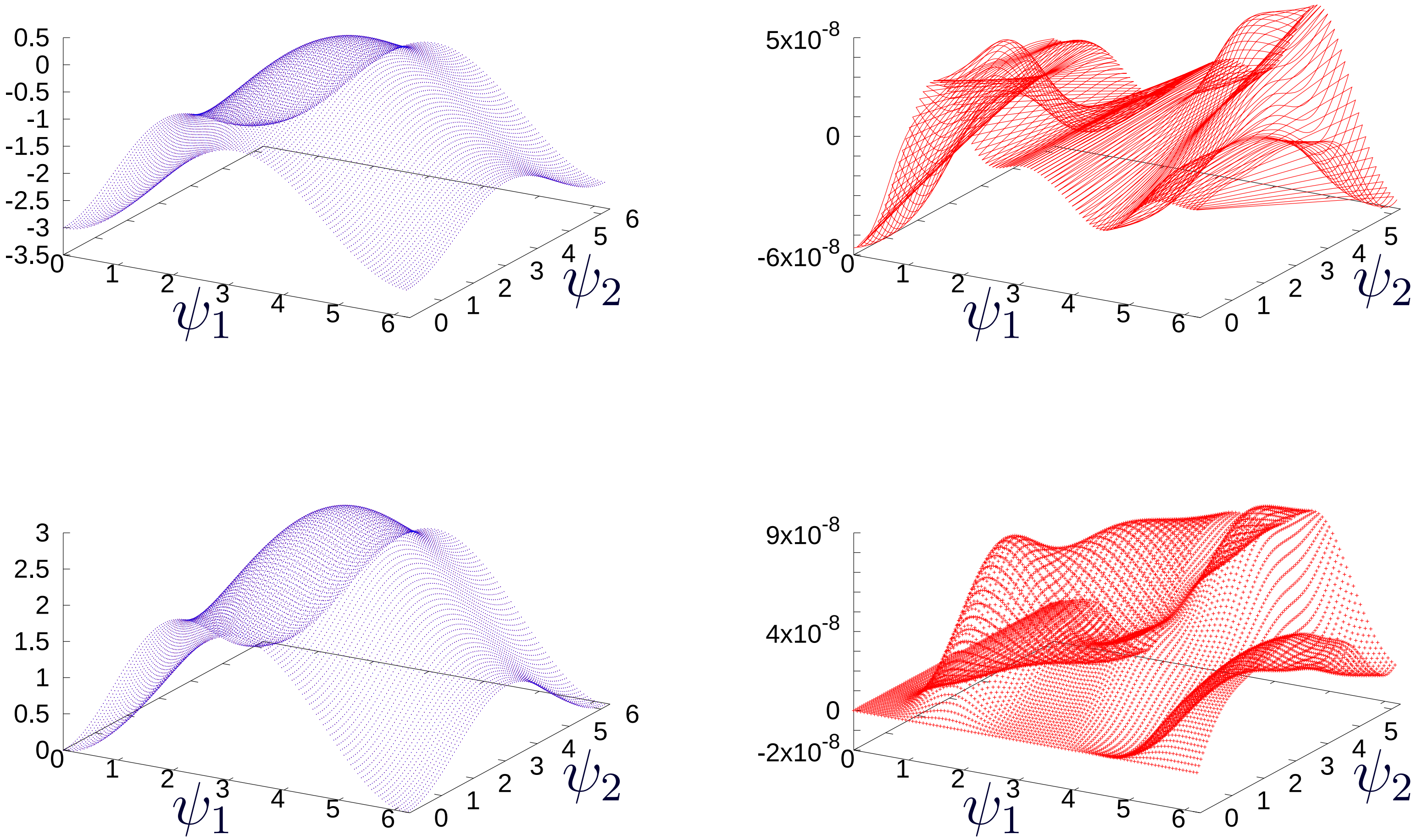

T_δ, $\delta = 0.2$. Left: h_{11} and $\tilde{h}_{11}$ of points $(\psi_1, \psi_2, 0, 0)$ with base point $p_0 = (\pi, \pi, 0, 0)$ (top) and $p_0 = (0, 0, 0, 0)$ (bottom). Right: Their difference.

h_n is an adiabatic invariant

Theorem (Gelfreich-V, 2018). Let $C > 0$ be a constant and $\gamma(x_b, x)$ be piecewise smooth paths such that $|\gamma(x_b, x)| \le C|x - x_b|$ for every $x \in D$. If a suspension of F_ϵ can be written in the form of a Hamiltonian vector field with a Hamiltonian function

$$H(t, x, \epsilon) = H_n^a(x, \epsilon) + \epsilon^{2n} H_n^b(t, x, \epsilon)$$

where the $\mathcal{C}^{2n+1}$ norms of H_n^a and H_n^b are bounded uniformly with respect ϵ and $H_n^a(x_b, \epsilon) = 0$, then for every compact $D_0 \subset D$ there is a constant C_n such that

$$\sup_{x \in D_0} |h_n(x, \epsilon) - H_n^a(x, \epsilon)| \le C_n \epsilon^{2n}$$

Corollary. For any compact $D_0 \subset D$ and $\forall x \in D_0$, one has

$$h_n(F_\epsilon(x), \epsilon) - h_n(x, \epsilon) = O(\epsilon^{2n}),$$

i.e. h_n is approximately preserved for ϵ^{-2n} iterates.

IVFs- "Poincaré" sections to visualize dynamics

Let $g : \mathbb{R}^m \to \mathbb{R}$ smooth s.t. $\Sigma = \{x \in \mathbb{R}^m : g(x) = 0\}$ is a smooth hyper-surface of codimension one.

Take $x_0 \in D$ and iterate $x_{k+1} = F_\epsilon(x_k)$. Assume that $g(x_k)g(x_{k+1}) \leq 0$ (crossing). If the limit vector field G_0 is (locally) transversal to Σ then, for ϵ small enough, there is a unique $t_k \in [0, \epsilon]$ such that $g(\Phi^{t_k}_{X_n}(x_k)) = 0$.

$\longrightarrow$ Plot $y_k = \Phi^{t_k}_{X_n}(x_k)$ instead of (any projection of) x_k.

Visualizing 4D near-Id dynamics: For a map like T_ϵ, obtained as a discretization of $H = J_1^2/2 + a_2 J_1 J_2 + a_3 J_2^2/2 + V(\psi)$, $\Sigma = \{\psi_1 = \psi_2\}$ is a transversal section (if $|\delta|$ small enough). On a moderate time scale the iterates of $x_0 \in \mathbb{T}^2 \times \mathbb{R}^2$ remain close to the "energy" surface $M^n_E = \{x : h_n(x, p_0) = E\}$, where $E = h_n(x_0, p_0)$. At each crossing, we project onto Σ along the IVF X_n to get $y_{k_j} \in \Sigma$.

For E large enough, one has $M^n_E \cong \mathbb{T}^3$. Then $\psi = \psi_1 = \psi_2$, $\phi = \arg(J_1 + iJ_2)$ are convenient coordinates on $\Sigma \cap M^n_E \cong \mathbb{T}^2$.

T_δ, $\delta = 0.35$, 400 *i.c. on* $\Sigma \cap \{h_{10} = 4\}$, 500 *it*

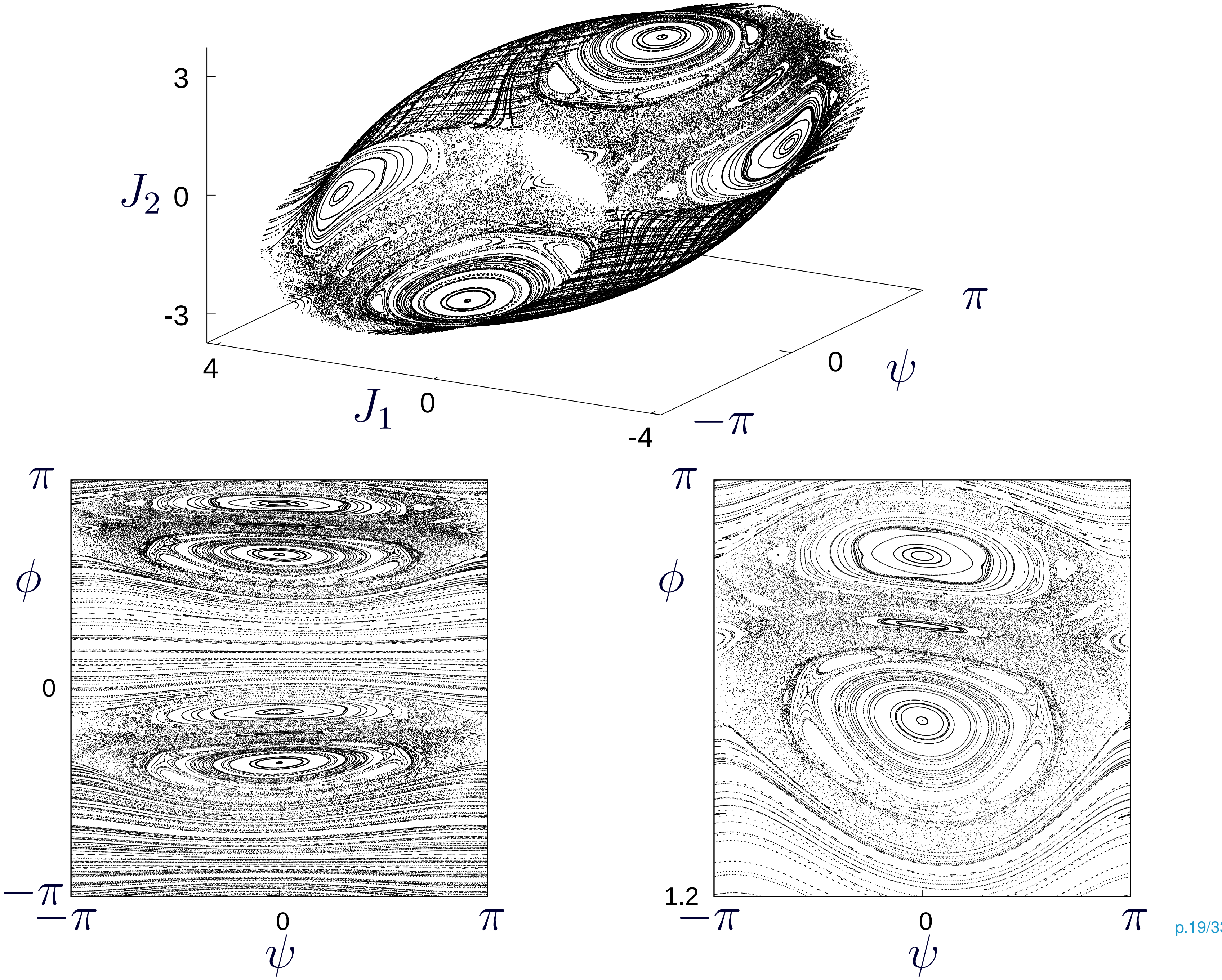

Exploring Arnold diffusion - covering

Lochak-Neishtadt $\Rightarrow \exists$ covering of the action space by neighbourhoods of the N-periodic orbits up to some period $N_{\max}$. In the corresponding neighbourhood F_ϵ^N becomes near-the-Id, hence we can use an IVF X_n to construct a slow variable h_n^N associated to such map.

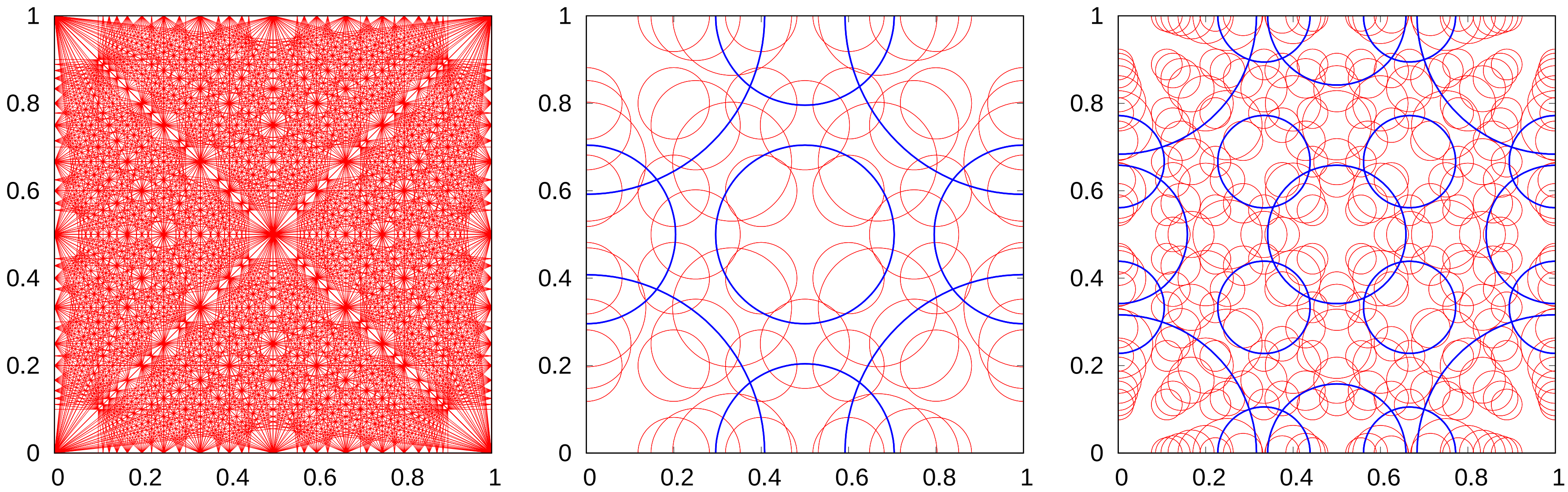

Left: resonant lines up to order 10 in frequency space. Center: We consider p.o. up to period $N_{\max} = 6$ and we plot a circle of radius $\frac{1}{N\sqrt{N_{\max}}}$ around. Right: Same for $N_{\max} = 10$. As $\epsilon \searrow 0$ more periods are needed. But to cover the resonances $(1,0)$ and $(0,1)$ we need periods $\ll N_{\max}$.

IVFs - covering

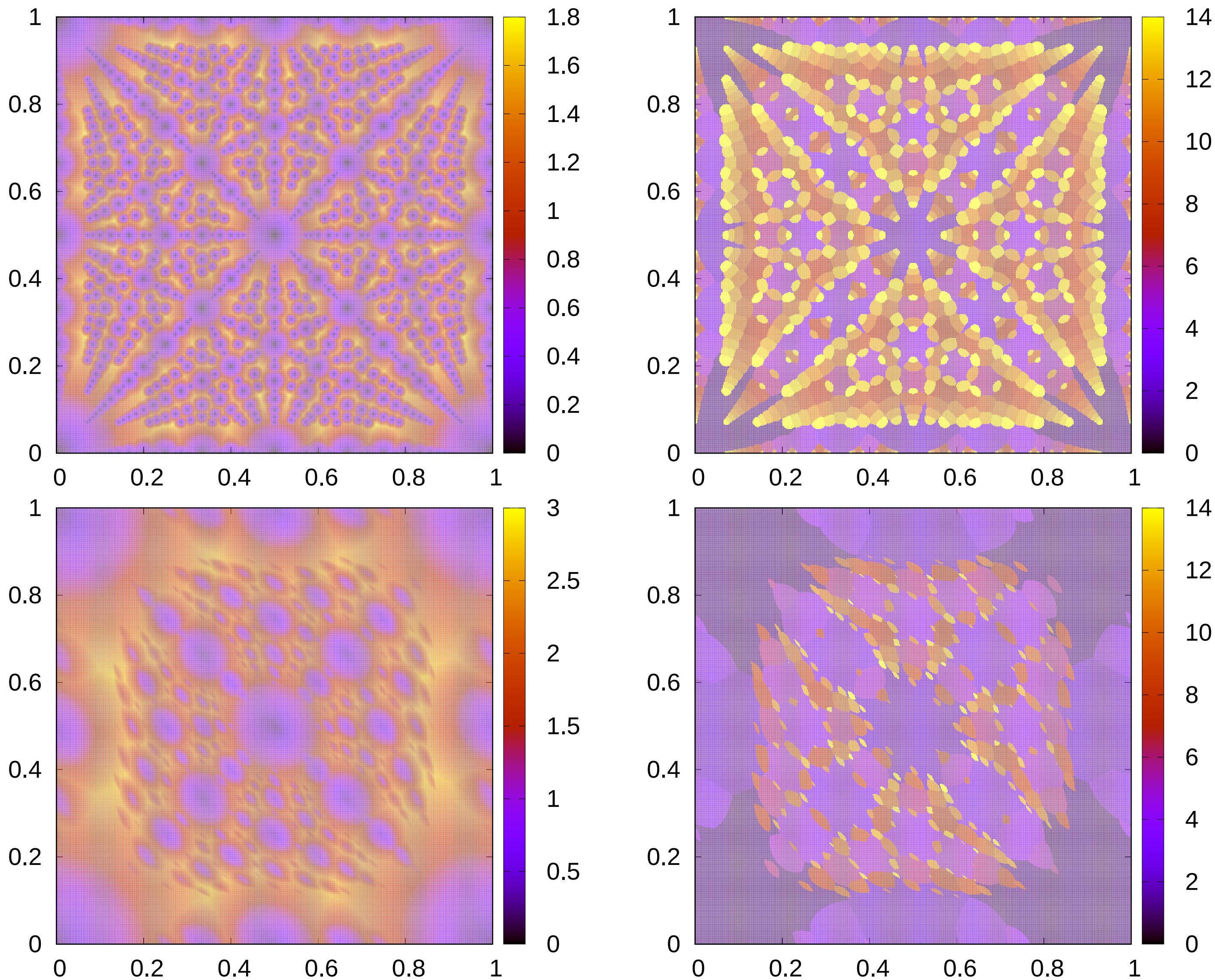

Integrable T_0

Left: dist-to-Id

Right: corresp. N

$T_\delta, \delta = 0.35$

Left: dist-to-Id

Right: corresp. N

For a fixed $\epsilon > 0$, the distance-to-Id of the map F^N increases as N increases, hence h_n^N has larger oscillations and it is preserved for less number of iterates.

Arnold diffusion - near double resonance

Near a double resonance that corresponds to p.o. of short period N, that is, near the junction of two resonant lines of small order, the distance-to-Id of F^N is small. Hence, h_n^N is well-preserved for a much larger number of iterates. This prevents orbits from getting close to or escaping from a small neighbourhood of the double resonance in a moderate number of iterates. We refer to the core of the double resonance.

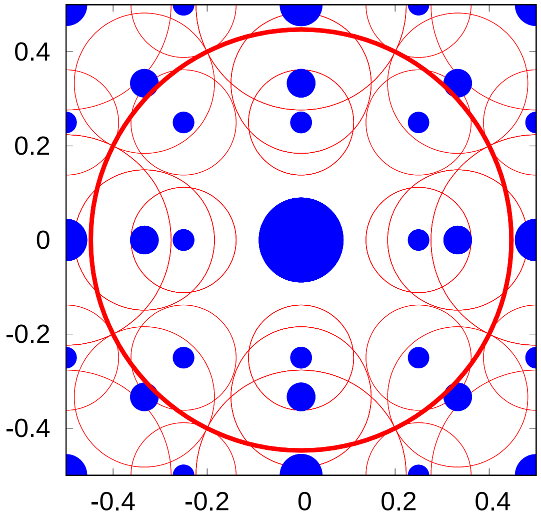

Qualitative picture, frequency space.

Assumption: The region between the covering radius (in red) and the core (blue disk) around the intersection of the main resonances $(1,0)$ and $(0,1)$ can be understood using h_n^1 and Poincaré sections.

Remark: Double resonances of different enough order, hence with large N, do not have core because h_n^N is badly preserved since F^N is far-from-Id.

Turning at a resonant crossing

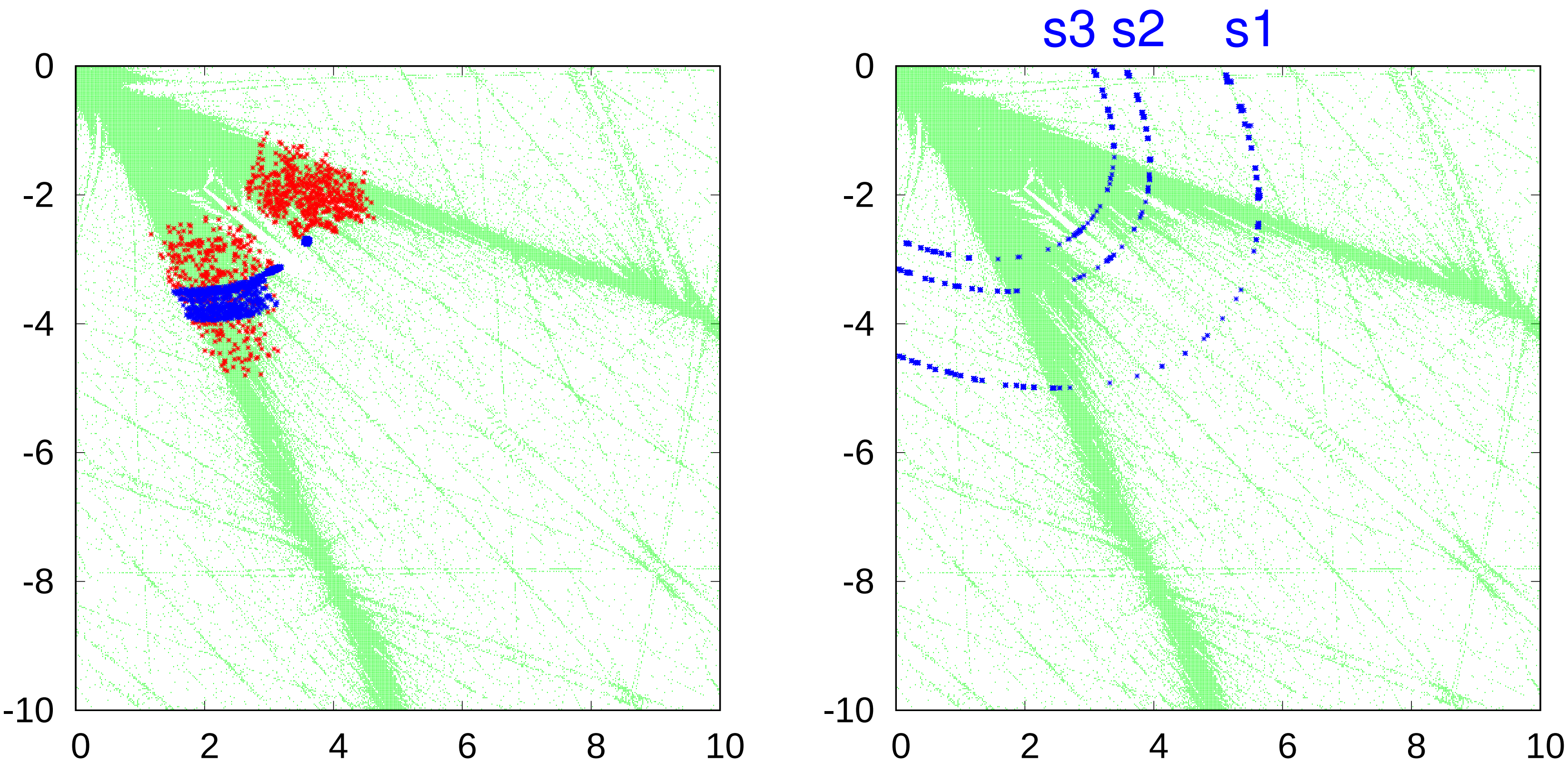

T_δ, $\delta = 0.4$. Left: IC $(3, 3, 2.136447, -3.904401)$ near $J_1 + a_2 J_2 \approx 0$. We perform around 10^8 (resp. 10^10) iterates and show in blue (resp. red) iterates on $\Sigma = \{\psi_1 = \psi_2\}$ with $|\psi_1 - \pi| < 0.35$. Similar for most orbits.

Right: Energy levels above the level of the crossing observed.

"Poincaré" sections & last "RIC"

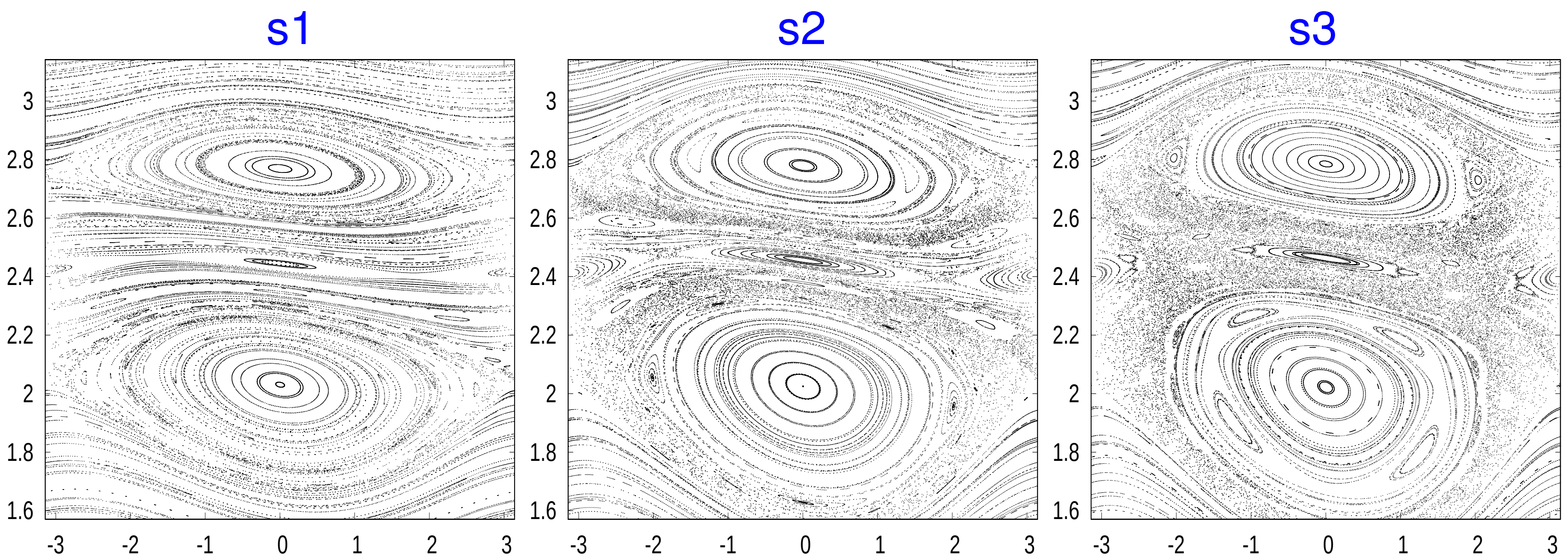

J_1	$\tilde{h}^1_{11}$	tori?
2.5	12.327	Y s1
2.0	7.889	Y
1.75	6.041	Y s2
1.625	5.209	N
1.5	4.439	N s3

Approaching the HH-point (with $h = 0$) of the double resonance the projection "Poincaré" maps become more chaotic. The last "rotational invariant curve" is at $h \approx h(\pi, \pi, J_1, -a_2 J_1) \approx 5.209$. It corresponds to $J_1 \approx 1.625$. Numerical simulations detect passages for $1.37 \lesssim J_1 \lesssim 1.5$.

Structure around double resonances

- Inside the core radius: the map F_ϵ^N is near-Id, h_n is well-preserved for longer times (large time scale, not observable), and the 2-dof approximation that defines the averaged system is chaotic.
- At the influence radius: the map F_ϵ^N is relatively far-from-Id, h_n is only well-preserved for relatively short times (medium time scale), and the 2-dof approximation that provide the averaged system is relatively close-to-integrable.

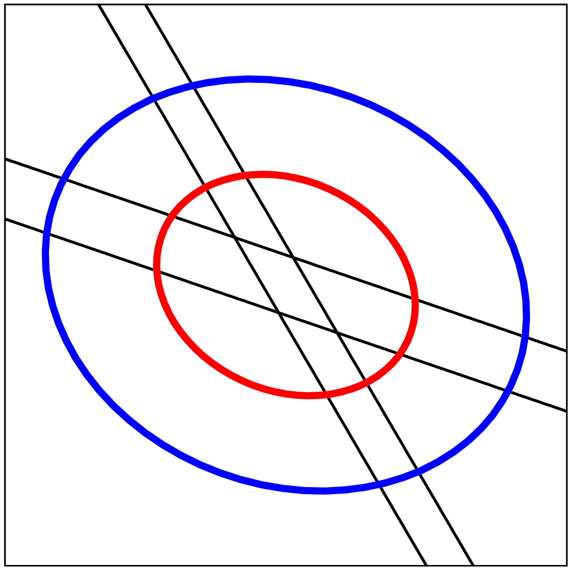

Turning/continue along a single resonance?

The situation observed at each double resonance changes with parameters. Consider an IC near the NHIC corresponding to a single resonance of small order, and that the iterates approach a double resonance. There is a hierarchy of time-scales where different phenomena takes place. The time-scale of the simulations corresponds to a medium time-scale and there is a much large time-scale which we cannot detect numerically (e.g. motion inside the core of a resonance). Depending on the distance-to-Id parameter ϵ of F^N around the double resonance we distinguish the following cases [a].

Case 1: For small values of ϵ the iterates can be only be reflected from the double resonance. No turning is allowed (within the simulation time scale).

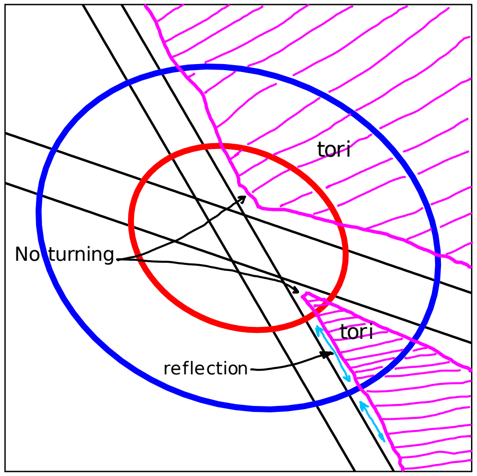

[a] For a concrete resonance, similar visualizations are obtained (case 2) implementing the changes of coordinates to get the averaged Hamiltonian, see C.Efthymiopoulos and M.Harsoula, *The speed of Arnold diffusion*, Physica D 25, 2013.

Turning/continue along a single resonance?

Case 2: This is the situation shown in the previous “Poincaré” plots for two resonances of similar order. Turning along the largest angle between the two resonances is not allowed (within the simulation time-scale).

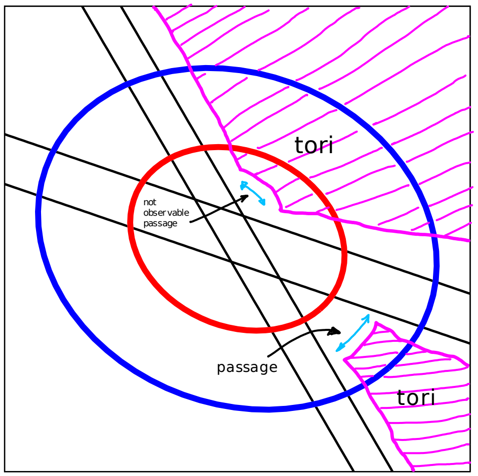

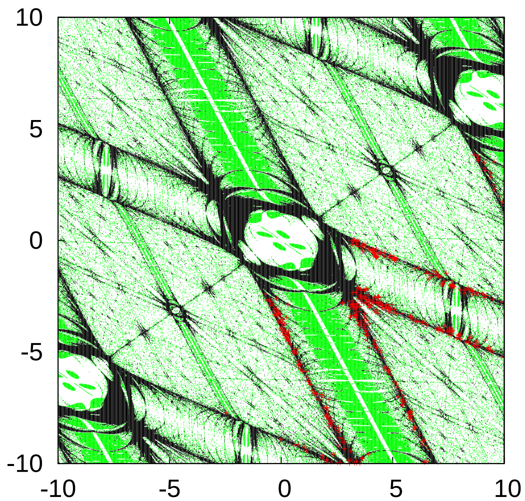

Case 3: For larger values of ϵ both turnings are possible, but with different probability. This is the situation for two resonances with different orders. Moving along the high-order single resonance is not observable in many cases because the distance-to-integrable decreases along it (for large N the core is small, and so is the influence radius). Note that the relative size of the core decreases.

Turning/continue along a single resonance?

Case 4: We cannot distinguish the level values of h_n where both passages take place. Both transitions take place with a similar probability. If the double resonances corresponds to the intersection of a low order with a high order single resonance then motion along the high-order one is not possible and, consequently, turnings are not observed. Points can be either reflected or can continue crossing the double resonance along the same single resonance. Both phenomena has similar probability. Moreover, increasing ϵ the core size is below the preservation threshold of h_n (that is, the core disappears).

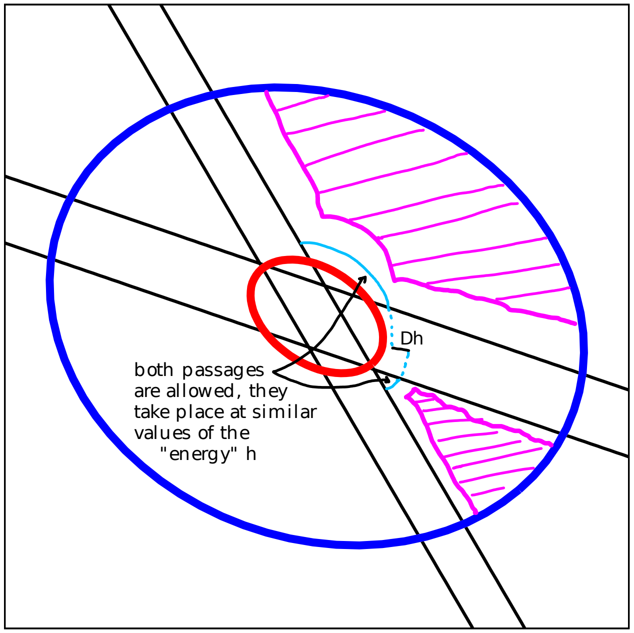

Remark. The dynamics at the h_n turning level is almost independent of the discretization parameter value, that is, when $\delta \searrow 0$ it converges to a non-integrable 2-dof Hamiltonian (highly chaotic) system. Properties of such limit dynamics (that depend for instance on the angle between resonances) determine the level at which the turning takes place.

Different crossings

We use a 4D map with a potential $V(\psi) = \frac{\cos(\psi_1)+\epsilon\cos(\psi_2)}{3(\cos(\psi_1)+\epsilon\cos(\psi_2)+3)}$, hence with all harmonics, an look at different resonances. Illustrations for $\delta = 0.2$.

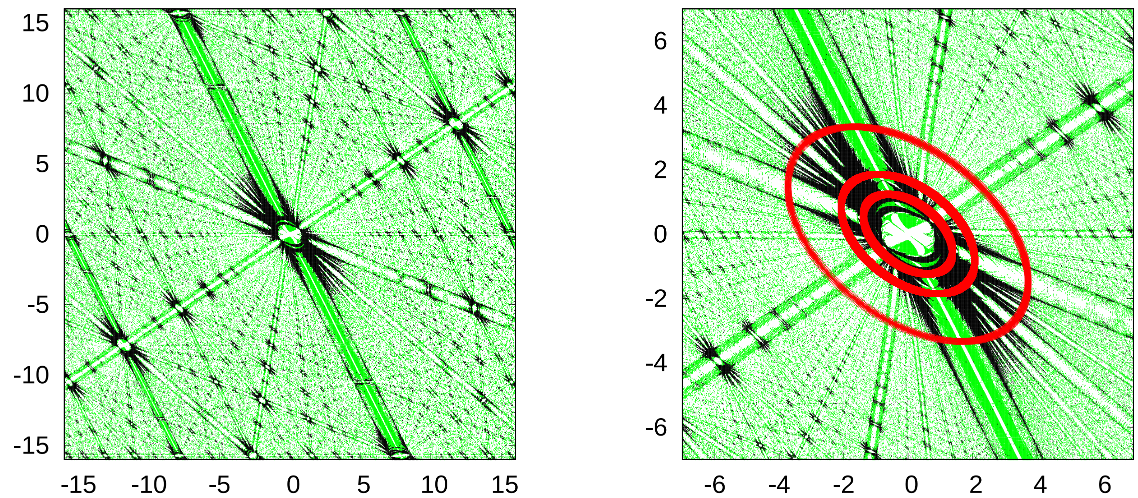

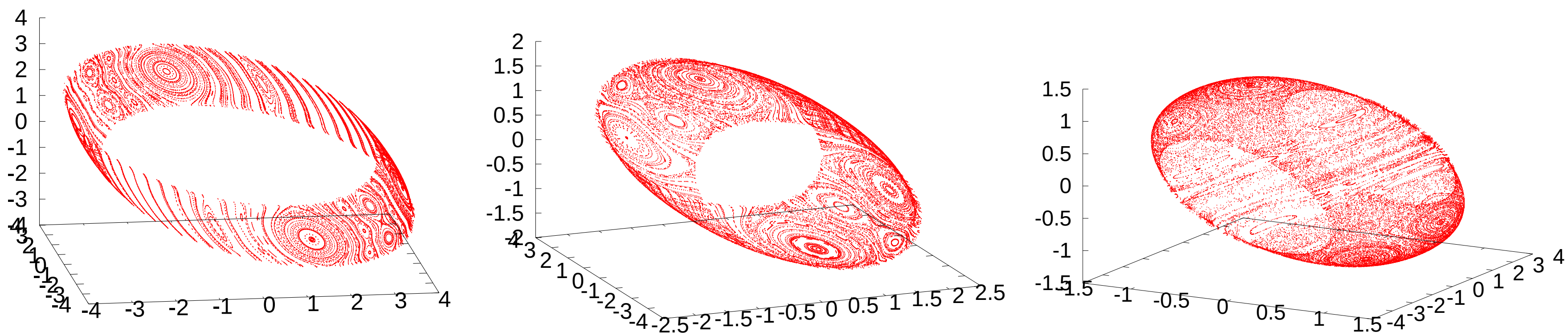

From left to right, "Poincaré" sections using $h^{N=1}$ and $J = 1.6,\ 0.8,\ 0.4$.

Different crossings

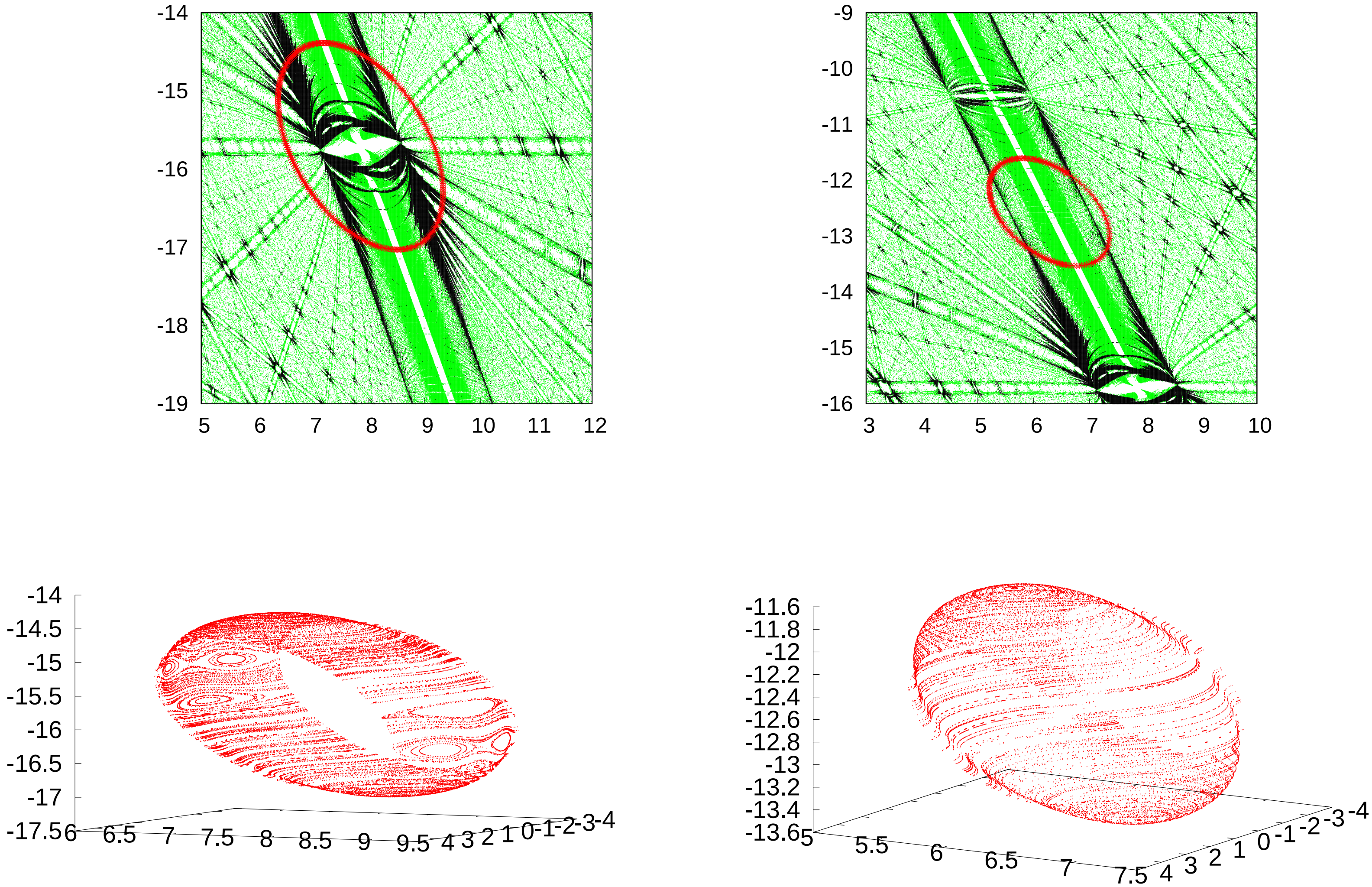

From left to right, “Poincaré” sections using $h^{N=2}$ (res 1:2, $J = 8.4$) and $h^{N=5}$ (res 2:5, $J = 6.6$)

Movie

Local diffusion along single resonances

We select 3×10^6 points close to the two hyperbolic points which correspond to the hyperbolic cylinders in $\Sigma \cap \{h_n = E\}$, for different E values. We iterate until $h_n = E \pm \Delta E$ (or until we reach 10^4 iterates). Results for T_δ, $\delta = 0.4$ and $\Delta E = 0.1$ (similar for other ΔE).

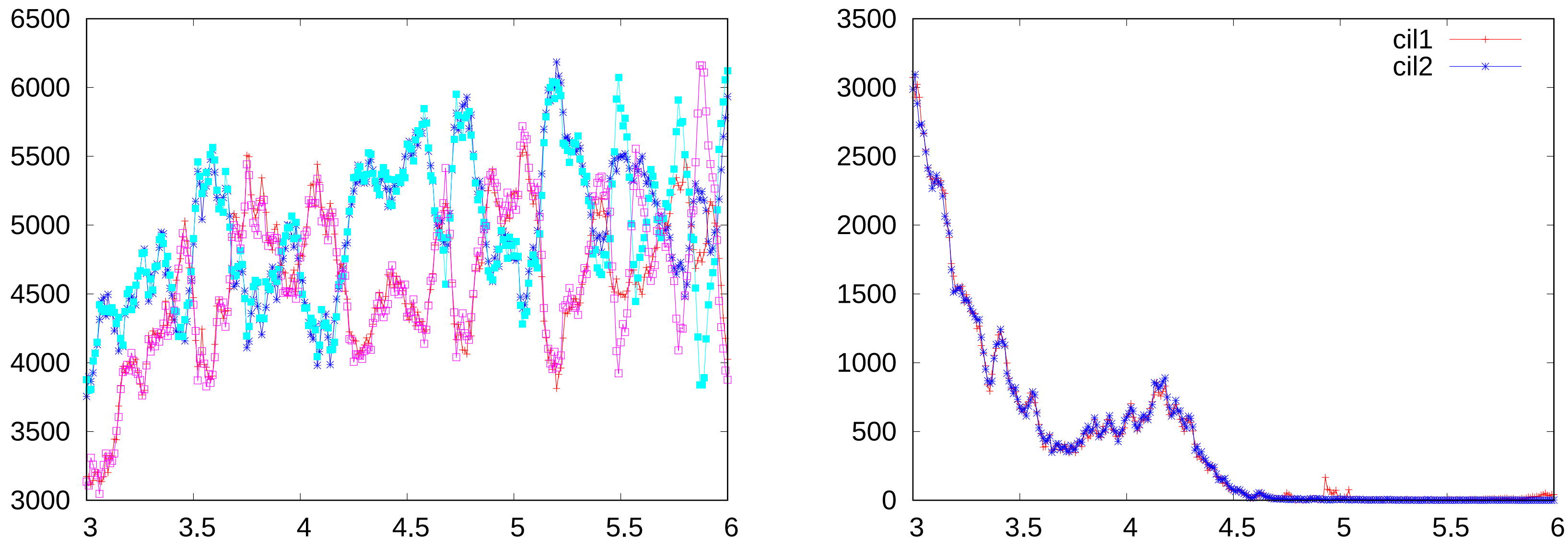

Left: Blue and light blue (resp. red and magenta): number of initial points in both cylinders that reach $E + \Delta E$ (resp. $E - \Delta E$).

Right: Number of initial points that do not reach $E \pm \Delta E$ in 10^4 iterates.

Local diffusive process

The oscillations of h_n along a single resonance are random-like.

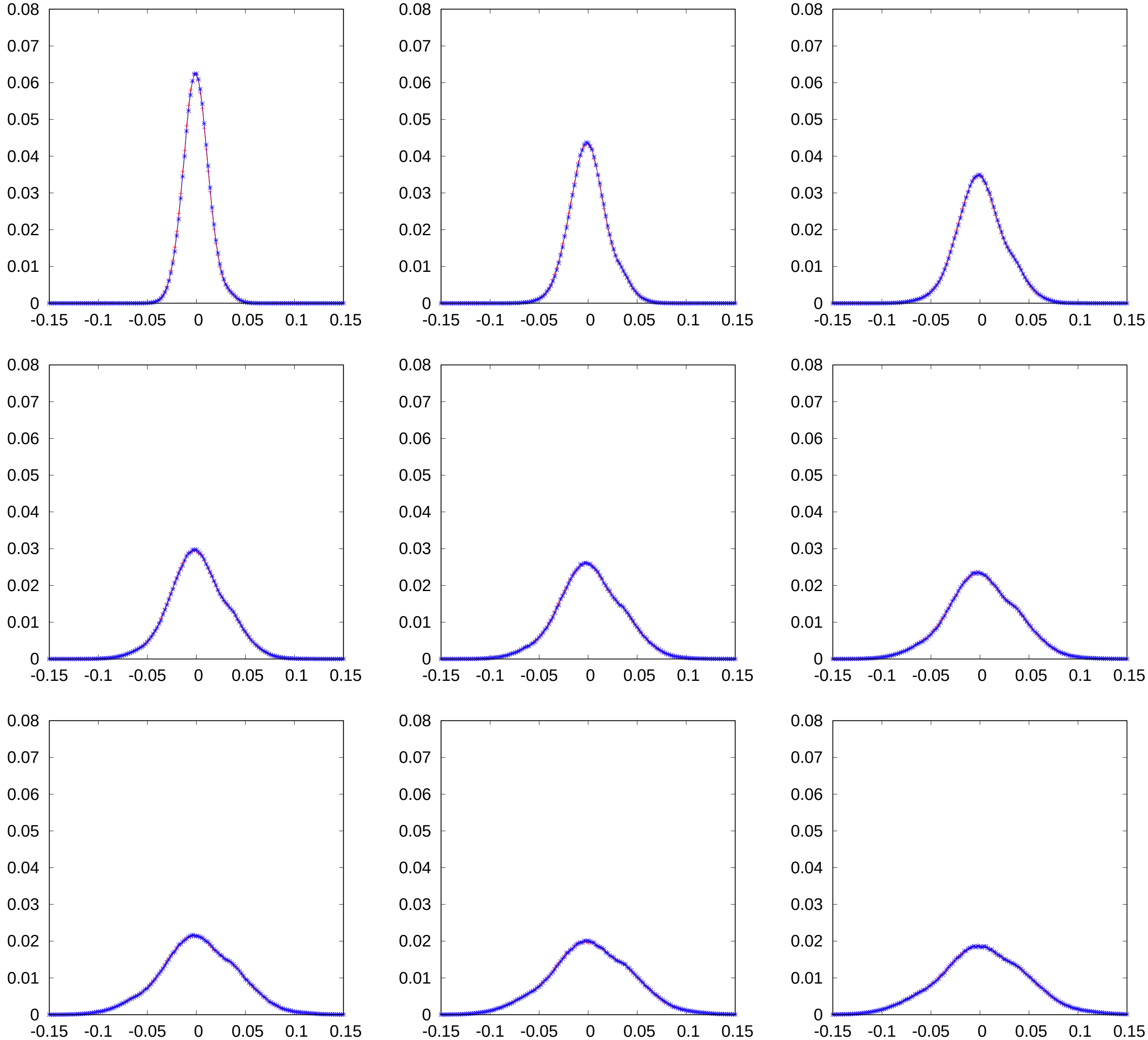

$\epsilon = 0.4,$

$h_n = 3.5,$

$N = 10^6$ i.c.,

$\texttt{nit} = k \cdot 10^6,$

$k = 1, \ldots, 9$

$\Downarrow$

Locally Gaussian

(but effect of many crossing resonances)

Outlook, conclusions & future work

- IVFs – a tool for exploring near-Id dynamics (useful in many other situations like 3D VPMs, dissipative systems, etc). We have used IVFs to investigate the key role of double resonances in the diffusion process of near-Id 4D symplectic maps. They are useful because:
  - IVFs give the averaged system avoiding the computations of the change of variables (we perform simulations in the original system variables).
  - IVFs give the slowest variable h_n at any point of the phase (useful for visualizations and effective computations of diffusion).
- Arnold diffusion, some questions we want to address:
  - Determine the optimal covering, describe how it changes wrt ϵ, and use it to get analytical estimates on the diffusion process.
  - Analytic estimates of the parameter ranges for which the different regimes at a double resonance are observed?
  - The stochastic limit needs to be clarified, and convergence to a local Gaussian process justified. Role of high order resonances?
  - Can we construct the "effective graph" of diffusion for a given IC (and for a given simulation time)? It must follow the resonant net on the complementary of KAM tori.

Thanks for your attention!!